Computational Assessment of Coronary Stent Performance: Structural and Hemodynamic Insights for Optimized Patient Outcomes

Alex Figueiredo[1], Ronny C Carbonari[1], Sônia M Malmonge[1], João Lameu[1]

[1]Federal University of ABC, São Bernardo do Campo, Brazil

Abstract

Coronary artery disease is a leading global cause of mortality, often treated by percutaneous coronary intervention with stent implantation. The long-term efficacy of this procedure is compromised by risks of in-stent restenosis and thrombosis, which are critically influenced by the stent's mechanical interaction with the artery and the subsequent hemodynamic environment. This study presents an integrated computational methodology to evaluate coronary stent performance by combining structural Finite Element Analysis (FEA) with Computational Fluid Dynamics. A parameterized model of a Nitinol stent, artery, and balloon was generated automatically using a custom Matlab algorithm. The stent's crimping, expansion via an ideal balloon and subsequent elastic recoil, incorporating realistic material properties was performed by FEA analysis. Results identified stress concentrations in stent struts and arterial wall. The deformed geometry was used for CFD analysis. The stent induced flow disturbances creating pro-atherogenic micro-environments: low time-averaged wall shear stress (TAWSS < 0.4 Pa), high oscillatory shear index (OSI > 0.25), and elevated relative residence time (RRT > 5 Pa^{-1}). The integrated approach provides a robust foundation for a systematic stent design in order to improve patient outcomes.

1. Introduction

Coronary artery disease (CAD) remains a leading global cause of morbidity and mortality, with rising prevalence linked to an aging population and increased risk factors such as diabetes and chronic kidney disease [1,2]. This has led to a greater number and complexity of percutaneous coronary interventions (PCI)[1]. PCI is a minimally invasive procedure used to restore blood flow in stenotic arteries in both acute and chronic CAD [2.3]. Stent implantation is central to PCI, with evolution from bare-metal to drug-eluting and bioresorbable platforms aimed at reducing restenosis and thrombosis [2,3]. However, complications such as in-stent restenosis, stent thrombosis, and neo-atherosclerosis persist, influenced by patient comorbidities, lesion characteristics, and procedural factors [2]. Ongoing innovation in stent design and materials continues to seek improvements in long-term safety and efficacy [3,4]. In this context, the main goal of the present paper is present an integrated approach of stent design, structural and hemodynamic analyses to evaluate the overall stent performance, that is crucial to provide detailed information about the stent implementation and its interaction of arterial walls with the blood flow, identifying areas of potential thrombosis risk or restenosis.

2. Methodology

The methodology presented in the article is divided into three parts: the first describes the geometric parameters; the second details the characteristics of the numerical model, such as the finite element mesh, the boundary conditions, and the parameters used in the solver; and finally, the CFD analysis.

2.1. Stent Design

The model shown in Figure 1 was systematically generated using a Matlab algorithm with the following input data: stent design and final diameter; artery diameter; ideal balloon diameter; stent and artery layer thicknesses; and stent geometry shape. Next, the same algorithm generates a finite element model with specified discretization for each part (the balloon, the stent, and the artery).

2.2. Structural Analysis

The structural analysis was divided into two parts representing the expansion and relaxation processes. First, the ideal balloon applies a uniform radial displacement to the stent until it reaches its final diameter. Then, the ideal balloon is removed to analyse the elastic recoil of the stent. Throughout these processes, the ends of the artery are fixed. Abaqus was used to solve the numerical model, considering the following conditions: friction between the balloon and the stent, between the stent and the artery, large deformations, and material nonlinearity. Due to the

time required to perform the expansion and relaxation processes, the solution was obtained using the implicit method for a quasi-static problem.

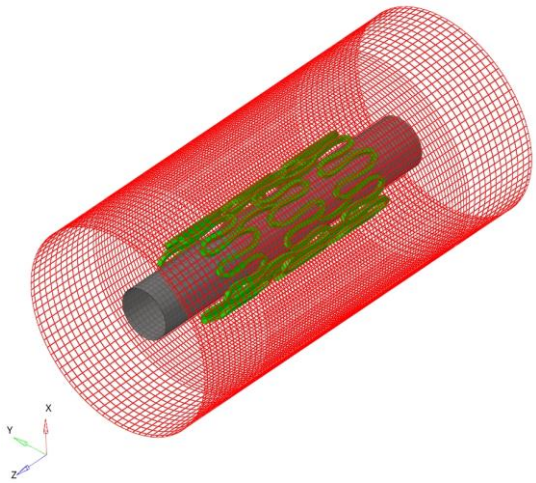


Figure 1. Computational model of the stent-artery-balloon system generated by the Matlab algorithm, including geometric discretization for each part.

2.3. Hemodynamic Analysis

A hybrid computational mesh composed of approximately 2.0 million elements, were generated from the 3D geometries. To solve accurately near-wall velocity gradients, 20 inflation layers were implemented with a first-layer thickness of 10 µm and a growth rate of 1.1 [5]. The Ansys CFD package was used. The Immersed Boundary Method was used to account for the stent structure in the fluid domain in Ansys CFX Solver. Also, the model incorporates laminar, incompressible, transient, isothermal flow with non-Newtonian blood rheology described by the Carreau-Yasuda model.

To evaluate the patient hemodynamic risk one case was simulated, considering stent implantation in an idealized Left Anterior Descending (LAD) of 4 mm diameter. Stenosis caused by atherosclerotic plaques was most frequently observed in the LAD, with an incidence of 77% [6]. For the hemodynamic model, the inlet boundary condition (BC) was defined as a transient, predominantly diastolic flow profile, with diastolic-to-systolic peak velocity ratio of 2.0 [7,8]. The outlet BC was defined by a model of coronary microcirculatory pressure [9], i.e., with a systolic pressure peak. In addition, the viscous blood-wall interaction was modelled as no-slip BC. A heart rate of 75 bpm (cardiac cycle: 0.8 s) was used, considering coronary flow of 5% of the total cardiac output (5 L/min).

For the numerical solution, the High-Resolution advection and the second-order Euler (Backward) schemes were employed with a residual target (RMS) of 1×10^{-4}. For each case, two complete cardiac cycles were simulated using a time step of 1×10^{-3} s and time-averaged values were obtained for the last cardiac cycle.

The assessment of hemodynamic predisposition to atherosclerosis was conducted through the quantification of Time-Averaged Wall Shear Stress (TAWSS)-based indicators: Oscillatory Shear Index (OSI) and Relative Residence Time (RRT). The OSI is a dimensionless metric that quantifies the cyclic deviation of the WSS vector direction from the time-averaged predominant flow direction. OSI ranges from 0, indicating unidirectional shear stress, to a theoretical maximum of 0.5, representing purely oscillatory shear stress. Elevated OSI values are hemodynamically linked to a pro-atherogenic endothelial phenotype. The RRT is a derived parameter that approximates the near-wall residence time of circulating particles. Prolonged RRT increases the probability of adhesion and transmigration of platelets and leukocytes across the endothelium. This can subsequently initiate a cascade of inflammatory responses and stimulate smooth muscle cell proliferation, both key mechanisms in the initiation and progression of atherosclerotic lesions. Comparative analyses have demonstrated that OSI and RRT exhibit superior positive predictive value, compared to TAWSS alone.

3. Results and Discussion

The numerical model considers a 4-mm-diameter coronary artery with an initial 2-mm-diameter stent and a 0.15-mm thickness. These measurements were obtained from [10,11].

3.1. Structural Analysis

The finite element meshes generated were structured, with the quantity for each part being: the stent has a total of 58,240 C3D8R elements; the balloon has a total of 2,112 M3D4R elements; and the artery has a total of 8,730 S4R elements. The expansion and relaxation times, as well as the material properties, were taken from [10,11].

Figure 2 shows the von Mises stress distributions at the end of balloon expansion (Figures 2a and 2b) and after it relaxes (Figures 2c and 2d). You can see that stress tends to concentrate mostly along the stent struts, and the arterial wall gets impacted more in areas where there's direct contact. After the balloon deflates, the stresses drop somewhat, but a few localized peaks are still noticeable. In Figure 3, you can see the radial displacement for both stages. The vessel experiences some elastic recovery, while the stent maintains its expanded shape.

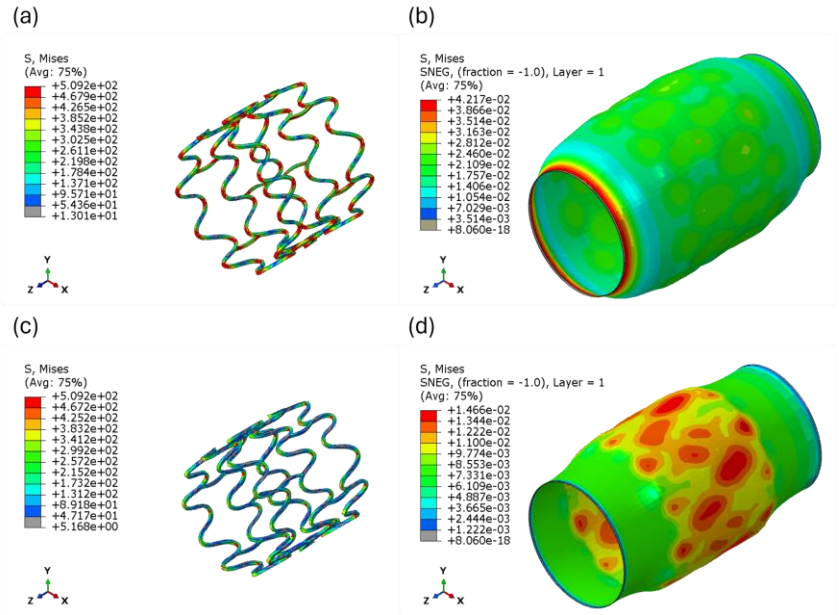


Figure 2. von Mises stress distribution at the end of balloon expansion: (a) stent and (b) arterial wall; and after relaxation: (c) stent and (d) arterial wall.

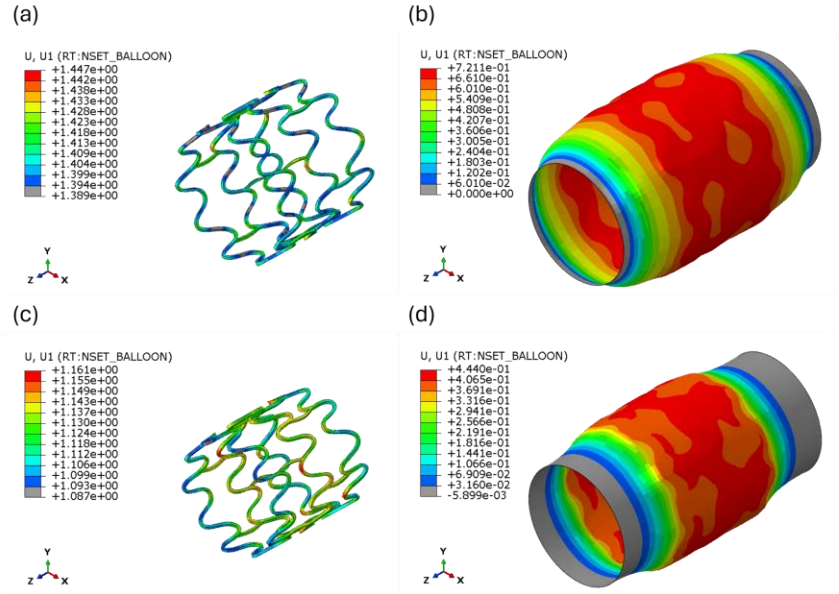


Figure 3. Radial displacement (UR) for balloon expansion: (a) stent and (b) arterial wall; and for relaxation: (c) stent and (d) arterial wall.

3.2. Hemodynamic Analysis

Figure 4 presents the TAWSS-based indicators along the vector field of blood velocity at diastolic peak for three cross sectional planes, being two inside the zone with stent implantation and one after the stent end.

The vector field of velocity (Figure 4-a,b) revealed flow disturbance inside the stent implantation zone at the diastolic peak, despite the laminar flow regime. This hemodynamic behaviour is directly related to the formation of small-scale vortices (Figure 4-b) and localized flow acceleration around the stent struts, which creates a microenvironment characterized by regions of oscillatory peaks (OSI > 0.25 Figure 4-d) and low wall shear stress (TAWSS < 0.4 Pa, Figure 4-c) and recirculation zones immediately downstream the stents, resulting in higher RRT (> 5 Pa^{-1}, Figure 4-e). Zones of low TAWSS combined with high OSI and RRT were correlated to thrombogenic-prone and neo-atherosclerotic incidence [5].

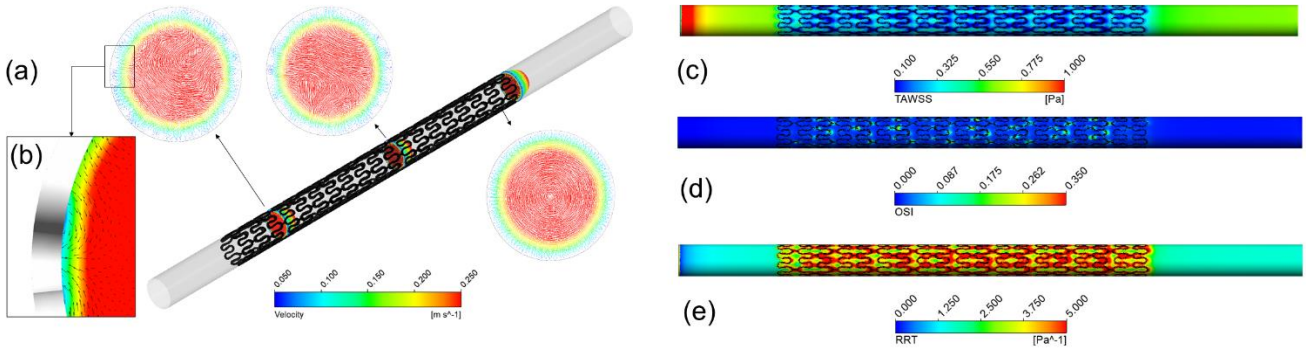


Figure 4. (a) Vector fields of blood velocity at diastolic peak for three cross-sectional planes, (b) details of velocity disturbance around the stent strut; (c) TAWSS, (d) OSI, (e) RRT.

4. Conclusion

This paper marks the beginning of developing a systematic methodology for designing stents by presenting a robust computational model. The major finding is that stent implantation creates localized hemodynamic disturbances—specifically low and oscillatory wall shear stress—that are directly linked to an increased risk of neo-atherosclerosis and thrombosis. While the presented model successfully identified these pro-atherogenic micro-environments, the methodology requires further improvement by incorporating steps like the crimping process and balloon expansion. The ultimate goal is to integrate this modelling approach with a shape optimization method. This will allow for the design of next-generation stents with geometries that minimize harmful hemodynamic effects and improve clinical outcomes.

Acknowledgments

This study was financed in part by the Coordenação de Aperfeiçoamento de Pessoal de Nível Superior - Brasil (CAPES) - Finance Code 001. The authors thank the financial support by CNPq (National Council for Scientific and Technological Development, Process 405055/2023-4).

References

[1] P. Lis, M. Rajzer, and Ł. Klima, "The significance of coronary artery calcification for percutaneous coronary interventions," Healthcare, vol. 12, no. 5, p. 520, 2024, doi: 10.3390/healthcare12050520.

[2] I. Hetherington and H. Totary-Jain, "Anti-atherosclerotic therapies: Milestones, challenges, and emerging innovations," Mol. Ther., vol. 30, pp. 3106-3117, 2022, doi: 10.1016/j.ymthe.2022.08.024.

[3] C. Pan, Y. Han, and J. Lu, "Structural design of vascular stents: a review," Micromachines, vol. 12, no. 7, p. 770, 2021, doi: 10.3390/mi12070770.

[4] A. Chernyak, M. Dzeshka, V. Snezhitskiy, A. Yanushka, and A. Maksimchik, "Percutaneous coronary interventions -- current state of development: Stents evolution," J. Grodno State Med. Univ., 2020, doi: 10.25298/2221-8785-2020-18-4-365-374.

[5] F. Gijsen et al., "Expert recommendations on the assessment of wall shear stress in human coronary arteries: existing methodologies, technical considerations, and clinical applications," Eur. Heart J., vol. 40, no. 41, pp. 3421-3433, 2019.

[6] K.S. Sakai et al., "Coronary atherosclerosis phenotypes in focal and diffuse disease," JACC: Cardiovasc. Imag., vol. 16, pp. 1452-1464, 2023, doi: 10.1016/j.jcmg.2023.05.018.

[7] A.G. Munneke, J. Lumens, T. Arts, and T. Delhaas, "A Closed-Loop Modeling Framework for Cardiac-to-Coronary Coupling," Front. Physiol., vol. 13, p. 830925, 2022.

[8] N. Hadjiloizou et al., "Differences in cardiac microcirculatory wave patterns between the proximal left mainstem and proximal right coronary artery," Amer. J. Physiol. Heart Circ. Physiol., vol. 295, p. H1198, 2008.

[9] P.H.M. Bovendeerd, P. Borsje, T. Arts, and F.N. van De Vosse, "Dependence of intramyocardial pressure and coronary flow on ventricular loading and contractility: a model study," Ann. Biomed. Eng., vol. 34, no. 12, pp. 1833-1845, Dec. 2006.

[10] J. Ha, J.S. Park, and C. Lee, "Finite element analysis of coronary stent deployment and evaluation of deployment characteristics according to plaque properties and geometries," Results Eng., vol. 26, 2025, doi: 10.1016/j.rineng.2025.105091.

[11] J.P. Toledo, J. Martínez-Castillo, D. Cardenas, E. Delgado-Alvarado, M.O. Vigueras-Zuñiga, and A.L. Herrera-May, "Simplified models to assess the mechanical performance parameters of stents," Bioengineering, vol. 11, no. 6, 2024, doi: 10.3390/bioengineering11060583.

João Lameu da Silva Jr.
Federal University of ABC (UFABC)
Alameda da Universidade, s/n, São Bernardo do Campo, Brazil
joao.lameu@ufabc.edu.br